Quantitative Analysis of Heat Release during Coal Oxygen-Lean Combustion in a $O_2/CO_2/N_2$ atmosphere by TG-DTG-DSC

Jingdong Shi
China University of Geosciences (Beijing)
Hetao Su (h.su@cugb.edu.cn)
China University of Geosciences (Beijing)
Yunzhuo Li
China University of Geosciences (Beijing)
Zijun Huang
China University of Geosciences (Beijing)
Yiru Wang
China University of Geosciences (Beijing)
Lintao Gao
China University of Geosciences (Beijing)

Research Article

Keywords: coal oxygen-lean combustion, multi-gas environment, heat release, apparent activation energy, quantitative analysis

Posted Date: February 16th, 2022

DOI: https://doi.org/10.21203/rs.3.rs-1352759/v1

Abstract

Coal combustion in an oxygen-lean and multi-gas environment is a common exothermic phenomenon for coalfield fires, leading to serious environmental destruction and loss of coal resources. Simultaneous thermal analysis experiments for Bulianta (BLT, high-volatile bituminous coal) and Yuwu coal (YW, anthracite) in 21vol.%O_2/79vol.%N_2 and 15vol.%O_2/5vol.%CO_2/80vol.%N_2 were carried out to study the law of heat release. Based on the TG-DTG-DSC curves, the combustion characteristic parameters were analyzed. A delay of ignition and heat release existed during the coal oxygen-lean combustion in O_2/CO_2/N_2. Decreasing O_2 concentration caused a significant reduction of local reactivity and further the decreasing maximum heat release rate for low-rank coal, while increasing CO_2 concentration caused a significant thermal lag effect and further the increasing maximum heat release rate for high-rank coal. The relationship between the heat release rate and the reaction rate constant was quantitatively analyzed. At the increasing stage of the heat release rate, the heat release rate of the two coals increased conforming to ExpGro1 exponential model. At the decreasing stage of the heat release rate, the heat release rate of YW coal decreased exponentially with the reaction rate constant, while the heat release rate of BLT coal decreased linearly. Regardless of the atmospheres, the conversion rates corresponding to maximum heat release rate of BLT and YW coal were about 0.80 and 0.50, respectively, indicating that the coal rank played a dominant role. The results are helpful to understand the heat release process of coal oxygen-lean combustion in O_2/CO_2/N_2.

1. Introduction

Coal is an important energy source to meet the power demand as well as to promote the economy development because of its abundant reserves [1–3]. Coalfield fires triggered by spontaneous coal combustion also occur continuously when mining, and are considered a global crisis, which not only causes serious environmental destruction and loss of coal resources, but also poses a serious threat to human safety and health. [4–7]. Most coalfield fires occur in an oxygen-lean (oxygen concentration lower than air) and multi-gas environment due to insufficient oxygen supply and combustion product gases [8]. The development and expansion of coalfield fires closely relate to the heat accumulation of coal combustion. Obtaining the law of heat release during coal oxygen-lean combustion in a multi-gas atmosphere will be beneficial to understand and reveal the dynamic spread of a coalfield fire.

Coalfield fires start from coal low-temperature oxidation. Pan et al. [2] studied the heat release of the oxidation characteristics of pulverized coal using a C600 microcalorimeter. The results showed that the oxidative heat evolution of pulverized coal has obvious stage characteristics of first absorbing heat and then releasing heat. Other scholars [9–12] also came to a conclusion consistent with the above. Chang et al. [13] investigated the oxidation pyrolysis of coal below 150℃ in Yangquan through a thermal analyzer. The results suggested that the low-temperature oxidation process was an obvious oxidation process of heat release compared with the pyrolysis process. Zhai et al. [14] used the derivative of heat flow with time to record the endothermic and heat release changes of coal samples at different heating rates. The results presented that a low heating rate promoted the heat release effects of coal oxidation, resulting in a more thorough heat release process. In addition, some scholars studied the low-temperature oxidation of coal in sections based on heat release. Li et al. [15] determined the intrinsic reaction of Ximeng lignite at low temperatures, and divided the intrinsic

reaction of coal and oxygen into three stages by using differential scanning calorimetry (DSC), including slow oxidation, accelerated oxidation, and rapid oxidation. The intrinsic reaction was to eliminate the heat release after water evaporation and thermal decomposition of internal oxygen-containing functional groups. The low-temperature oxidation of coal was also divided into water loss and weight loss stage, oxygen absorption stage and thermal decomposition stage by some scholars for research [16]. Totally, how to detect and prevent coalfield fires in the low-temperature oxidation stage of coal are the purpose of most scholars' research.

Exploring the overall heat release process of coal combustion is beneficial to understand the coalfield fires. Deng et al. [17] investigated the gas production and thermal behavior of weathered coal and fresh coal. The heat released by weathered coal continued to maintain oxidation under high temperature and oxygen-lean conditions. Su et al. [18] studied the main characteristic behaviors (temperature gradient, oxygen consumption, oxidation kinetics, gaseous products and heat release) of coal combustion, and divided the evolution process into five stages. Zhao et al. [19] divided the high-temperature oxidation process into four stages through using thermogravimetric differential scanning calorimetry (TG-DSC), including water evaporation and gas desorption, oxygen absorption and weight gain, thermal decomposition and combustion, and obtained detailed heat release characteristics. Most of research in the above was aimed at O_2/N_2 and O_2/CO_2 atmospheres. Because of the lower heat conduction coefficient and lower diffusivity of CO_2 than N_2, when N_2 in the atmosphere was completely replaced with CO_2 under the general supply in O_2/N_2, the reaction rate decreased, and the ignition and combustion delayed and the time to reach burnout extended [20–28]. Wang et al. [29] found that the TG curves of coal and coke combustion in O_2/CO_2 tended to be higher temperature range compared with conventional combustion. This was in accordance with the research results of Cahyadi et al. [30] and Ren et al. [12]. The above-mentioned studies only focused on the ignition, burnout, and weightlessness delay, the heat release of coal oxygen-lean combustion was not studied in details. As the O_2 concentration gradually decreased in the O_2/N_2 or O_2/CO_2 atmospheres, the heat release rate decreased and delayed, the coal combustion slowed down and the burnout time extended [10–12, 29]. The heat release process was not only affected by insufficient oxygen supply, it was also corrected with the presence of CO_2, H_2O, etc., when coalfield fires were in the oxygen-lean environment with multi-gas components such as $O_2/CO_2/N_2$, $O_2/N_2/H_2O$, $O_2/H_2O/CO_2$, etc. [31–34].

Heat release is the basis of coalfield fire spreading. However, there are currently few studies on the heat release of coal oxygen-lean combustion in a multi-gas environment. The purpose of this work is to analyze the law of heat release during coal oxygen-lean combustion in a $O_2/CO_2/N_2$ atmosphere. Simultaneous thermal analysis experiments were carried out for two coal samples in 21vol.%O_2/79vol.%N_2 and 15vol.%O_2/5vol.%CO_2/80vol.%N_2, respectively. Based on the TG-DTG-DSC curves, the combustion characteristic parameters were discussed, and the kinetic parameters were obtained. Furthermore, the relationship between the exothermic rate and the reaction rate constant was proposed. This work can provide theoretical support for revealing the spread of coalfield fires.

2. Experiments And Methods

2.1 Preparation of coal samples

Two fresh coal samples were selected from the Bulianta colliery in Inner Mongolia and the Yuwu colliery in Shanxi, China, denoted as BLT and YW, respectively. The reason for choosing these two kinds of coal is that they belong to different rank coals and can show good experimental results. BLT coal belongs to high-volatile bituminous coal, which has a higher volatile matter (31.66%), lower fixed carbon (43.30%) and higher ash content (16.16%) than that of YW coal. YW coal belongs to anthracite. Coal samples were crushed in the laboratory, then sieved through 0.60mm, 0.45mm and 0.30mm gauze. The particle size between 0.30 ~ 0.45mm were selected as the experimental coal samples. The proximate analysis and ultimate analysis had been carried out in our previous research [35], as shown in Table 1.

Table 1
Proximate analysis and ultimate analysis of coal samples [35]

Coal sample	Proximate analysis (ad, %)				Ultimate analysis (ad, %)				
	Moisture	Ash	Volatile matter	Fixed Carbon	Nitrogen	Carbon	Hydrogen	Sulfur	Oxygen
BL coal	8.88	16.16	31.66	43.30	0.94	63.44	5.08	0.28	15.03
YW coal	0.71	9.40	9.90	79.99	1.30	83.48	4.05	0.24	3.72

2.2 TG-DTG-DSC experiment

A synchronous thermal analyzer (NETZSCH STA 449 F3) was utilized. Two atmospheres, including 21vol.%O_2/79vol.%N_2 and 15vol.%O_2/5vol.%CO_2/80vol.%N_2 were set up. The coal sample was put in a container. Gases passed into the container from two inlets, one of which located the bottom with a gas flow rate of 50ml/min and another one located the middle with a gas flow rate of 20ml/min. Two kinds of coal samples, with a mass of about 13mg were heated from room temperature to 1100°C, at three heating rates of 10°C/min, 15°C/min, and 20°C/min, respectively, as seen in Table 2. Based on the synchronous thermal analyzer, the schematic diagram of the experimental system is shown in Fig. 1.

Table 2
Experimental design

Experiment number	Atmosphere	Heating rate (°C/min)	Heating range (°C)
BLT 1	O_2/N_2	10	room temperature ~ 1100
BLT 2	O_2/N_2	15	
BLT 3	O_2/N_2	20	
BLT 4	$O_2/CO_2/N_2$	10	
BLT 5	$O_2/CO_2/N_2$	15	
BLT 6	$O_2/CO_2/N_2$	20	
YW 1	O_2/N_2	10	
YW 2	O_2/N_2	15	
YW 3	O_2/N_2	20	
YW 4	$O_2/CO_2/N_2$	10	
YW 5	$O_2/CO_2/N_2$	15	
YW 6	$O_2/CO_2/N_2$	20	

2.3 combustion kinetic theory

The coal combustion kinetic equation can be expressed as follows [36]

$$\frac{d\alpha}{\mathrm{d}t} = k(T) \cdot f(\alpha)$$

1

Where, *k(T)* is the reaction rate constant. *α* corresponds to the conversion of coal, its expression is as follows

$$\alpha = \frac{W_{\mathrm{O}} - W\mathrm{i}}{W_{\mathrm{O}} - W_{\infty}}$$

2

Where, W_{i} means the coal mass corresponding to the time of *i*.

The reaction rate constant of coal combustion can be expressed as follows [37].

$$k(T) = A\exp\left(-\frac{E}{\mathrm{R}T}\right)$$

3

Where, A corresponds to the pre-exponential factor (min^{-1}); E corresponds to the apparent activation energy (kJ/mol), R corresponds to the universal gas constant.

The kinetics equation of non-isothermal reaction can be expressed as follows [38]

$$\frac{\mathrm{d}\alpha}{\mathrm{d}T} = \frac{A}{\beta}\exp(-\frac{E}{\mathrm{R}T})f(\alpha)$$

4

Where, β corresponds to the heating rate for non-isothermal experiments.

Due to the high accuracy, the Kissinger-Akahira-Sunose (KAS) method was utilized to calculate the apparent activation energy. Its expression is as follows

$$\ln\left(\frac{\beta}{T_\alpha{}^2}\right) = \ln\left[\frac{AR}{Eg(\alpha)}\right] - \frac{E}{\mathrm{R}T}$$

5

Based on the plot of $\ln(\beta/T_\alpha{}^2)$ versus 1000/T, activation energies were calculated from the slope of the linear regression lines, pre-exponential factors were estimated from the intercepts.

3. Results And Discussions

3.1 The influence of the $O_2/CO_2/N_2$ atmosphere on the combustion characteristic parameters

Figure 2 gives the calculation method of combustion characteristic parameters, including ignition temperature (T_i), maximum heat release rate (v_p) and the temperature corresponding to maximum heat release rate (T_p). T_i corresponds to the temperature which coal samples begin to burn, and its value reflects the propensity of coal to spontaneous combustion. (T_p, v_p) is the point that the heat release rate of coal reaches to the maximum. It shows as the valley point on the DSC curve. The corresponding results are shown in Table 3. When the heating rate was constant, the values of T_i and T_p in the $O_2/CO_2/N_2$ atmosphere visibly increased compared with that in the O_2/N_2 atmosphere. This indicated that a delay of ignition and heat release existed during coal oxygen-lean combustion in the $O_2/CO_2/N_2$ atmosphere. This result was consistent with the literature [34–35, 39–40].

In the $O_2/CO_2/N_2$ atmosphere, the values of v_p for BLT coal samples decreased by 2.55 mW/mg, 4.18 mW/mg, and 16.51 mW/mg at 10°C/min, 15°C/min, and 20°C/min, respectively, compared with that in the O_2/N_2 atmosphere, because the decreasing O_2 concentration leaded to a reduction of local reactivity [28]. The values of v_p for YW coal samples increased by -3.52 mW/mg, 1.43 mW/mg, and 4.25 mW/mg at 10°C/min, 15°C/min, and 20°C/min, respectively, because the lower heat conduction coefficient of CO_2 than N_2 caused a thermal lag effect [41]. It can be seen that the influence of the $O_2/CO_2/N_2$ atmosphere on the maximum heat

release rate was restricted by the coal rank. The low-rank coal burned faster due to its low carbon content, and O_2 had a significant impact on the maximum heat release rate. The high-rank coal contained more carbon and burned slowly, and CO_2 had a significant impact on the maximum heat release rate.

Table 3
Characteristic temperatures of BLT and YW coal

Experiment number	T_i (°C)	T_p (°C)	V_p (mW/mg)
BLT 1	401.16	491.94	32.75
BLT 2	394.45	522.18	41.01
BLT 3	370.52	539.18	45.36
BLT 4	431.16	521.05	30.20
BLT 5	425.75	549.20	36.83
BLT 6	385.53	573.96	28.85
YW 1	513.40	568.39	24.84
YW 2	519.18	608.91	26.68
YW 3	529.82	641.79	29.74
YW 4	530.42	598.98	21.32
YW 5	546.19	636.54	28.11
YW 6	544.22	654.27	35.99

3.2 The influence of the $O_2/CO_2/N_2$ atmosphere on the kinetic parameters by KAS method

Figure 3 shows the changes in the values of apparent activation energy and correlation coefficients (R^2) by KAS method, in the two atmospheres. For BLT coal, as the conversion rate increased, the values of apparent activation energy all first decreased, then increased, and finally decreased. In the range of 0.5 ~ 0.15 conversion rate, it was in the low-temperature oxidation process. Since the R^2 was lower than 0.80, the values of apparent activation energy were not accurate and cannot be compared. When the conversion rate was higher than 0.15, the coal sample was ignited, and the values of apparent activation energy values in the two atmospheres appeared a sudden increase. During the combustion process, the values of apparent activation energy in the $O_2/CO_2/N_2$ atmosphere were approximately 33%~58% lower than that in the O_2/N_2 atmosphere. This was because the heat released by coal combustion accumulated more easily in the $O_2/CO_2/N_2$ atmosphere than in the O_2/N_2 atmosphere, as a result of the reduction of 6 vol.% O_2 and the addition of 5 vol.% CO_2 (low heat conduction coefficient).

For YW coal, as the conversion rate increased, the values of apparent activation energy in the two atmospheres kept decreasing. When the conversion rate was 0.05, it was in the low-temperature oxidation

process, and the values of apparent activation energy in the $O_2/CO_2/N_2$ atmosphere were approximately 40% higher than that the O_2/N_2 atmosphere. This has been confirmed in the research of others [25, 35]. When the conversion rate was higher than 0.05, the coal was ignited, and the values of apparent activation energy in the two atmospheres were close. The influence of the atmosphere was no longer obvious.

In addition, the R^2 in the two atmospheres was greater than 0.99. However, for BLT coal, a decrease behavior was showed in the conversion rates ranges of 0.10 ~ 0.25 in O_2/N_2 and 0.15 ~ 0.45 in $O_2/CO_2/N_2$, respectively. The reason was that the precipitation of the remaining volatiles was promoted by the heat release of separated volatiles combustion [28, 42–43], and the precipitation and combustion of volatile was significantly deferred in the $O_2/CO_2/N_2$ atmosphere compared with that in the O2/N2 atmosphere, as a result of the slightly lower diffusivity of volatiles in CO_2 than in N_2 [28, 44–45] and the lower mass flux of oxygen to the volatiles flame [28, 46].

3.3 The influence of the $O_2/CO_2/N_2$ atmosphere on the heat release

The reaction rate between oxygen and coal is the key factor influencing the heat release rate [47]. Studying the relationship between the heat release rate and reaction rate is beneficial to understand in the heat release process during coal oxygen-lean combustion in the $O_2/CO_2/N_2$ atmosphere, which can provide a theoretical foundation for revealing the law of coalfield fire spreading. Since the value of the reaction rate constant can directly reflect the reaction rate, the reaction rate constant was used instead of the reaction rate in this study. According to our previous research [35], the kinetic mechanism functions of BLT and YW coal were Jander (Diffusional (3-D)) and three-level chemical reaction, respectively. The values of pre-exponential factor were calculated though Eq. (5), and then the values of reaction rate constant were obtained though Eq. (3).

Figure 4 and 5 show the DSC-k(T) curves of BLT and YW coal, respectively. The conversion rate corresponding to the maximum heat release rate was taken as a segment point, and the DSC-k(T) curves were divided into two stages: the increasing stage and the decreasing stage of the heat release rate. The conversion rate corresponding to the maximum heat release rate of BLT and YW coal was always about 0.80 and 0.50, respectively., indicating that the conversion rate corresponding to the maximum heat release rate was only related to the coal rank, and not corrected to the atmosphere.

At the increasing stage of the heat release rate, the heat release rate of two coals increased exponentially with the increasing reaction rate constant. At the decreasing stage of the heat release rate, the heat release rate of YW coal decreased exponentially with the increasing reaction rate constant, whereas the heat release rate of BLT coal decreased linearly with the increasing reaction rate constant. This was because the ash on the coal surface obviously hindered the continued diffusion of O_2 into the coal pores, resulting in a decrease in the subsequent heat release rate. BLT coal contained less carbon and less ash, so its heat release rate decreased more slowly than that of YW coal and decreased linearly with the increasing reaction rate constant. ExpGro1 exponential model (see Eq. (6)) was selected to fit the DSC-k(T) curves at the increasing stage of heat release rate for the two coal samples. The model showed a high degree of fit, with the R^2 for both BLT and YW coal sample above 0.94. Therefore, the relationship between the heat release rate and reaction rate constant for

both BLT and YW coal sample can be effectively expressed by the model. The relationship between the heat release rate and the reaction rate constant is approximately as Eq. (7).

$$y = y_0 + A_1 \exp \frac{x}{t_1}$$

6

$$|\mathrm{DSC}| = y_0 + A_1 \exp \frac{\mathrm{d}\alpha/\mathrm{d}t}{t_1 f(\alpha)}$$

7

Where, y_0 is the offset. A_1 is the amplitude, t_1 is the width.

In order to quantitatively analyze the relationship between y_0, A_1 and t_1 and heating rate, Figs. 6 and 7 show the changes in y_0, A_1 and t_1 with the heating rate, respectively. There was a linear relationship between y_0, A_1, t_1 and heating rate for YW coal. For BLT coal, y_0, A_1 and t_1 were basically linear with the heating rate in the O_2/N_2 atmosphere, whereas there was a non-linear relationship between y_0, A_1, t_1 and heating rate in the $O_2/CO_2/N_2$ atmosphere. Furthermore, y_0-β, y_0-A_1 and y_0-t_1 curves were fitted respectively. The reaction rate constant was calculated using Eq. (1). On the whole, there was a following relationship between the heat release rate and reaction rate of coal, as follows

$$|\mathrm{DSC}| = a_1\beta + b_1 + (a_2\beta + b_2) \times \exp \frac{\mathrm{d}\alpha/\mathrm{d}t}{\left(a_3\beta + b_3\right) f(\alpha)}$$

8

Where, a_1 and b_1 are constants related to y_0, a_2 and b_2 are constants related to A_1, a_3 and b_3 are constants related to t_1, as seen in Table 4.

Table 4
The value of constants in equation. (8)

Coal samples	Atmosphere	Conversion rate range	a_1	b_1	a_2	b_2	a_3	b_3
BLT	O_2/N_2	0.05–0.80	1.59	20.78	-1.67	-13.35	-0.09	0.19
		0.80–0.95	1.28	21.04	-0.04	0.83	/	/
YW	O_2/N_2	0.05–0.50	0.33	22.12	0.08	-25.54	-0.00	-0.01
		0.50–0.95	0.75	0.84	-0.35	21.32	-0.42	2.89
	$O_2/CO_2/N_2$	0.05–0.50	1.47	6.42	-1.23	-12.41	-0.00	0.00
		0.50–0.95	1.31	-4.48	0.05	13.32	-0.42	3.07

4. Conclusions

In this work, simultaneous thermal analysis experiments for BLT coal (high-volatile bituminous coal) and YW coal (anthracite) in the 21%O_2/79%N_2 and 15%O_2/5%CO_2/80%N_2 atmospheres were carried out. Based on the TG-DTG-DSC curves, the combustion characteristic parameters were discussed, the values of apparent activation energy were obtained using Coats-Redfern method, and the relationship between the heat release rate and reaction rate constant was quantitatively analyzed. The following conclusions can be drawn:

(1) A delay of ignition and heat release existed during the coal oxygen-lean combustion in $O_2/CO_2/N_2$. Decreasing O_2 concentration caused a significant reduction of local reactivity and further the decreasing maximum heat release rate for low-rank coal, while increasing CO_2 concentration caused a significant thermal lag effect and further the increasing maximum heat release rate for high-rank coal.

(2) During the combustion process, the values of apparent activation energy in the $O_2/CO_2/N_2$ atmosphere were approximately 33%~58% lower than that in the O_2/N_2 atmosphere for BLT coal, while the values of apparent activation energy in the two atmospheres for YW coal were close. For BLT coal, the values of correlation coefficients were less than 0.80 in the conversion rates ranges of 0.10 ~ 0.25 in O_2/N_2 and 0.15 ~ 0.45 $O_2/CO_2/N_2$, respectively, which was because that the precipitation of the remaining volatiles was promoted by the heat release of separated volatiles combustion, and the precipitation and combustion of volatile was significantly deferred in the $O_2/CO_2/N_2$ atmosphere compared with that in the O_2/N_2 atmosphere due to the slightly lower diffusivity of volatiles in CO_2 than in N_2 and the lower mass flux of oxygen to the volatiles flame.

(3) Regardless of the atmospheres, the conversion rates corresponding to maximum heat release rate of BLT and YW coal were about 0.80 and 0.50, respectively, indicating that the coal rank played a dominant role. At the increasing stage of the heat release rate, the heat release rate of the two coals increased conforming to ExpGro1 exponential model. At the decreasing stage of the heat release rate, the heat release rate of YW coal decreased exponentially with the reaction rate constant, while the heat release rate of BLT coal decreased linearly.

Declarations

Acknowledgments

This work is supported by the National Natural Science Foundation of China [52004257], the 111 Project [B17041], and the Fundamental Research Funds for the Central Universities [2652018098].

References

1. Zhu J, Ouyang Z, Lu Q, Numerical simulation on pulverized coal combustion and NOx emissions in high temperature air from circulating fluidized bed, Journal of Thermal Science 22 (2013) 261–268.
2. Pan R, Qiu T, Chao J, Ma H, Wang J, Li C, Thermal evolution of the oxidation characteristics of pulverized coal with different particle sizes and heating rates, Thermochimica Acta 685 (2020) 178516.
3. O. Edenhofer, King coal and the queen of subsidies, Science 349 (2015) 1286–1287.

4. Carras JN, Young BC, Self-heating of coal and related materials: models, application and test methods, Prog Energy Combust 20 (1994) 1–15.
5. Fierro V, Miranda JL, Romero C, Andres JM, Arriaga A, Schmal D, Visser GH, Prevention of spontaneous combustion in coal stockpiles: experimental results in coal storage yard, Fuel Process Technol 59 (1999) 23–34.
6. Green U, Aizenshtat Z, Metzger L, Cohen H, Field and laboratory simulation study of hot spots in stockpiled bituminous coal, Energy Fuels 26 (2012) 7230–7235.
7. He-tao Su, Fu-bao Zhou, Bo-bo Shi, Hai-ning Qi, Jin-chang Deng, Causes and detection of coalfield fires, control techniques, and heat energy recovery: A review, International Journal of Minerals, Metallurgy and Materials 27 (2020) 275–291.
8. Stracher GB, Modern and Ancient Coal Fires in the Powder River Basin, Wyoming and Montana. Coal Peat Fires: A Global Perspective (2019) 71–89.
9. Zhang, Yanni, Yunchao Hou, Jingyu Zhao, Jun Deng, Xinyu Wen, Chunhui Liu, Anpeng Wang and Pan Shu, Heat Release Characteristic of Key Functional Groups During Low-Temperature Oxidation of Coal, J Combustion Science and Technology 193 (2020) 2692–2703.
10. Ren L-F, Deng J, Li Q-W, Ma L, Zou L, Laiwang B, et al, Low-temperature exothermic oxidation characteristics and spontaneous combustion risk of pulverised coal, Fuel 252 (2019) 238–245.
11. Deng J, Ren L-F, Ma L, Lei C-K, Wei G-M, Wang W-F, Effect of oxygen concentration on low-temperature exothermic oxidation of pulverized coal, Thermochimica Acta 667 (2018) 102–10.
12. Ren L-F, Li Q-W, Deng J, Yang X, Ma L, Wang W-F, Inhibiting effect of CO_2 on the oxidative combustion thermodynamics of coal, RSC Advances 9 (2019) 41126–41134.
13. Lu C, Zheng Y-m, Yu M-g, Research on low-temperature oxidation and pyrolysis of coal by thermal analysis experiment, Procedia Earth and Planetary Science 1 (2009) 718–723.
14. Zhai X, Ge H, Shu C-M, Obracaj D, Wang K, Laiwang B, Effect of the heating rate on the spontaneous combustion characteristics and exothermic phenomena of weakly caking coal at the low-temperature oxidation stage, Fuel 268 (2020) 117327.
15. Li Z, Zhang Y, Jing X, Zhang Y, Chang L, Insight into the intrinsic reaction of brown coal oxidation at low temperature: Differential scanning calorimetry study, Fuel Processing Technology 147 (2016) 64–70.
16. Deng J, Wang K, Zhang Y, Yang H, Study on the kinetics and reactivity at the ignition temperature of Jurassic coal in North Shaanxi, Journal of Thermal Analysis and Calorimetry 118 (2014) 417–423.
17. Deng J, Song J-J, Zhao J-Y, Zhang Y-N, Zhang Y-X, Shu C-M, Gases and thermal behavior during high-temperature oxidation of weathered coal, Journal of Thermal Analysis and Calorimetry 138 (2019) 1573–1582.
18. Su H, Ji H, Chen X, Model simplification of coal combustion kinetics: a case study of Weihuliang coal in Urumchi, China, Combustion Theory and Modelling 23 (2019) 1071–1089.
19. Zhao J, Deng J, Chen L, Wang T, Song J, Zhang Y, et al, Correlation analysis of the functional groups and exothermic characteristics of bituminous coal molecules during high-temperature oxidation, Energy 181 (2019) 136–147.

20. Zheng Y, Li Q, Zhang G, Zhao Y, Zhu P, Ma X, et al, Effect of multi-component gases competitive adsorption on coal spontaneous combustion characteristics under goaf conditions, Fuel Processing Technology 208 (2020) 106510.
21. Shen Z, Zhang L, Liang Q, Xu J, Lin K, Liu H, In situ experimental and modeling study on coal char combustion for coarse particle with effect of gasification in air (O_2/N_2) and O_2/CO_2 atmospheres, Fuel 233 (2018) 177–187.
22. Zhang L, Wu D, Cai L, Zou C, Qiu J, Zheng C, The chemical and physical effects of CO_2 on the homogeneous and heterogeneous ignition of the coal particle in O_2/CO_2 atmospheres, Proceedings of the Combustion Institute 36 (2017) 2113–2121.
23. Zhang L, Binner E, Qiao Y, Li C-Z, In situ diagnostics of Victorian brown coal combustion in O_2/N_2 and O_2/CO_2 mixtures in drop-tube furnace, Fuel 89 (2010) 2703–2712.
24. Qiao Y, Zhang L, Binner E, Xu M, Li C-Z, An investigation of the causes of the difference in coal particle ignition temperature between combustion in air and in O_2/CO_2, Fuel 89 (2010) 3381–3387.
25. Deng J, Ren L-F, Ma L, Qin X-Y, Wang W-F, Liu C-C, Low-temperature oxidation and reactivity of coal in O_2/N_2 and O_2/CO_2 atmospheres, a case of carboniferous–permian coal in Shaanxi, China, Environmental Earth Sciences 78 (2019) 234.
26. Bu C, Pallarès D, Chen X, Gómez-Barea A, Liu D, Leckner B, et al, Oxy-fuel combustion of a single fuel particle in a fluidized bed: Char combustion characteristics, an experimental study, Chemical Engineering Journal 287 (2016) 649–656.
27. Bu C, Liu D, Chen X, Pallarès D, Gómez-Barea A, Ignition behavior of single coal particle in a fluidized bed under O_2/CO_2 and O_2/N_2 atmospheres: A combination of visual image and particle temperature, Applied Energy 115 (2014) 301–308.
28. Shaddix CR, Molina A, Particle imaging of ignition and devolatilization of pulverized coal during oxy-fuel combustion, Proceedings of the Combustion Institute 32 (2009) 2091–2098.
29. Wang Ca, Zhang X, Liu Y, Che D, Pyrolysis and combustion characteristics of coals in oxyfuel combustion, Applied Energy 97 (2012) 264–273.
30. Cahyadi, Surjosatyo A, Nugroho YS, Predicting Behavior of Coal Ignition in Oxy-fuel Combustion, Energy Procedia 37 (2013) 1423–1434.
31. Bu C, Gómez-Barea A, Leckner B, Wang X, Zhang J, Piao G, The effect of H_2O on the oxy-fuel combustion of a bituminous coal char particle in a fluidized bed: Experiment and modeling, Combustion and Flame 218 (2020) 42–56.
32. Lei M, Sun C, Zou C, Mi H, Wang C, Effect of H_2O on the NO emission characteristics of pulverized coal during oxy-fuel combustion, Environmental science and pollution research international 25 (2018) 11767–11774.
33. Lei M, Zou C, Xu X, Wang C, Effect of CO_2 and H_2O on the combustion characteristics and ash formation of pulverized coal in oxy-fuel conditions, Applied Thermal Engineering 133 (2018) 308–315.
34. Tolvanen H, Raiko R, An experimental study and numerical modeling of combusting two coal chars in a drop-tube reactor: A comparison between N_2/O_2, CO_2/O_2, and $N_2/CO_2/O_2$ atmospheres, Fuel 124 (2014)

190–201.

35. Su Hetao, Kang Ning, Shi Bobo, Ji Huaijun, Li Yunzhuo, Shi Jingdong, Simultaneous thermal analysis on the dynamical oxygen-lean combustion behaviors of coal in a $O_2/CO_2/N_2$ atmosphere, Journal of the Energy Institute 96 (2021) 128–139.
36. Keuleers RR, Janssens JF, Desseyn HO, Comparison of some methods for apparent activation energy determination of thermal decomposition reactions by thermogravimetry, Thermochimica Acta 385 (2002) 127–142.
37. Jones JC, Chiz PS, Koh R, Matthew J, Kinetic parameters of oxidation of bituminous coals from heat-release rate measurements, Fuel 75 (1996) 1755–1757.
38. Jones JC, Henderson KP, Littlefair J, Rennie S, Kinetic parameters of oxidation of coals by heat-release measurement and their relevance to self-heating tests, Fuel 77 (1998) 19–22.
39. Barzegar R, Yozgatligil A, Atimtay AT, Combustion characteristics of Turkish lignites at oxygen-enriched and oxy-fuel combustion conditions, Journal of the Energy Institute 92 (2019) 1440–1450.
40. Li Q, Zhao C, Chen X, Wu W, Li Y, Comparison of pulverized coal combustion in air and in O_2/CO_2 mixtures by thermo-gravimetric analysis, Journal of Analytical and Applied Pyrolysis 85 (2009) 521–528.
41. Wen-hao Huangfu et al, Effects of Oxygen Concentrations and Heating Rates on Non-isothermal Combustion Properties of Jet Coal in East China, Procedia Engineering 211 (2018) 262–270.
42. Juan Riaza, Reza Khatami, Yiannis A. Levendis, Lucía Álvarez, María V. Gil, Covadonga Pevida, Fernando Rubiera, José J. Pis, Single particle ignition and combustion of anthracite, semi-anthracite and bituminous coals in air and simulated oxy-fuel conditions, Combustion and Flame 161 (2014) 1096–1108.
43. Reza Khatami, Yiannis A. Levendis, An overview of coal rank influence on ignition and combustion phenomena at the particle level, Combustion and Flame 164 (2016) 1–13.
44. Reza Khatami, Chris Stivers, Kulbhushan Joshi, Yiannis A. Levendis, Adel F. Sarofim, Combustion behavior of single particles from three different coal ranks and from sugar cane bagasse in O_2/N_2 and O_2/CO_2 atmospheres, Combustion and Flame 159 (2011) 1253–1271.
45. Sheng Qi, Zhihua Wang, Mário Costa, Yong He, Kefa Cen, Ignition and combustion of single pulverized biomass and coal particles in N_2/O_2 and CO_2/O_2 environments, Fuel 283 (2021) 118956.
46. Yang Xu, Shuiqing Li, Qi Gao, Qiang Yao, and Jianmin Liu, Characterization on ignition and volatile combustion of dispersed coal particle streams: in-situ diagnostics and transient modelling, Energy Fuels 32 (2018) 9850–9858.
47. Hui-Fei Lü, Yang Xiao, Jun Deng, Da-jiang Li, Lan Yin, Chi-Min Shu, Inhibiting effects of 1-butyl-3-methyl imidazole tetrafluoroborate on coal spontaneous combustion under different oxygen concentrations, Energy 186 (2019) 115907.

Figures

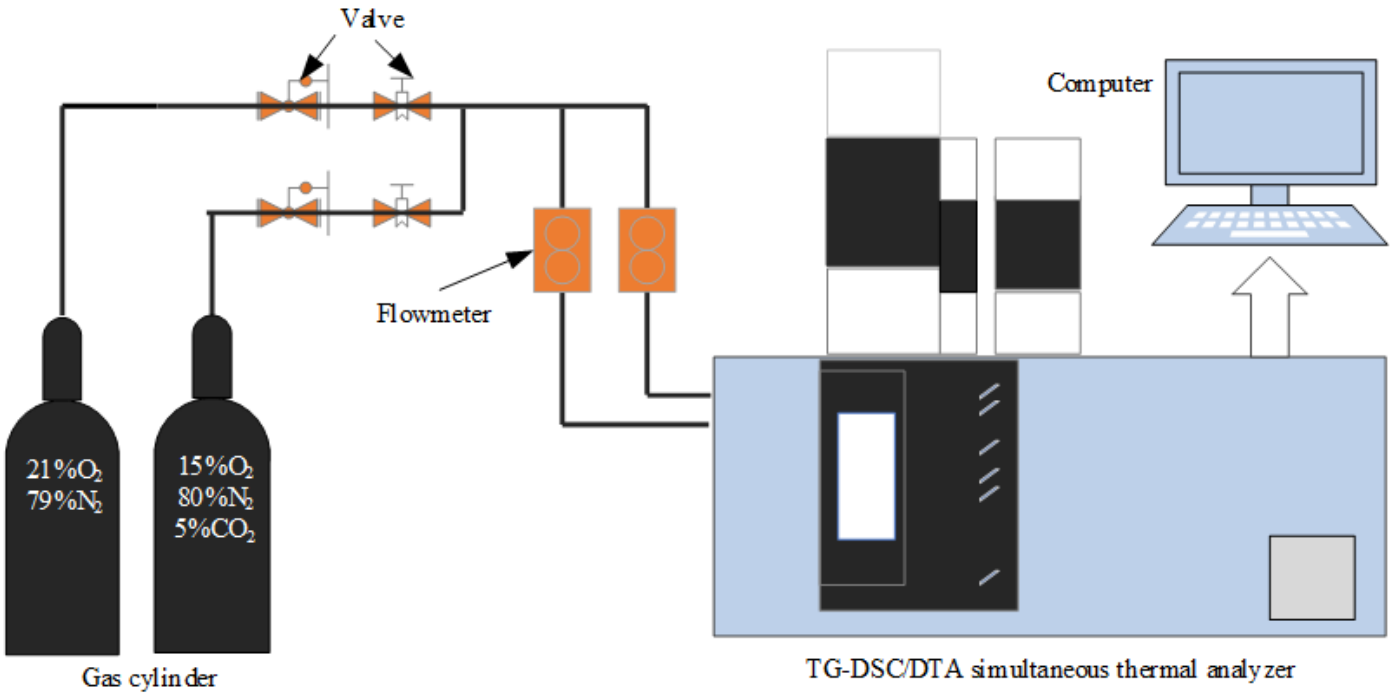

Figure 1

Schematic diagram of the experimental system

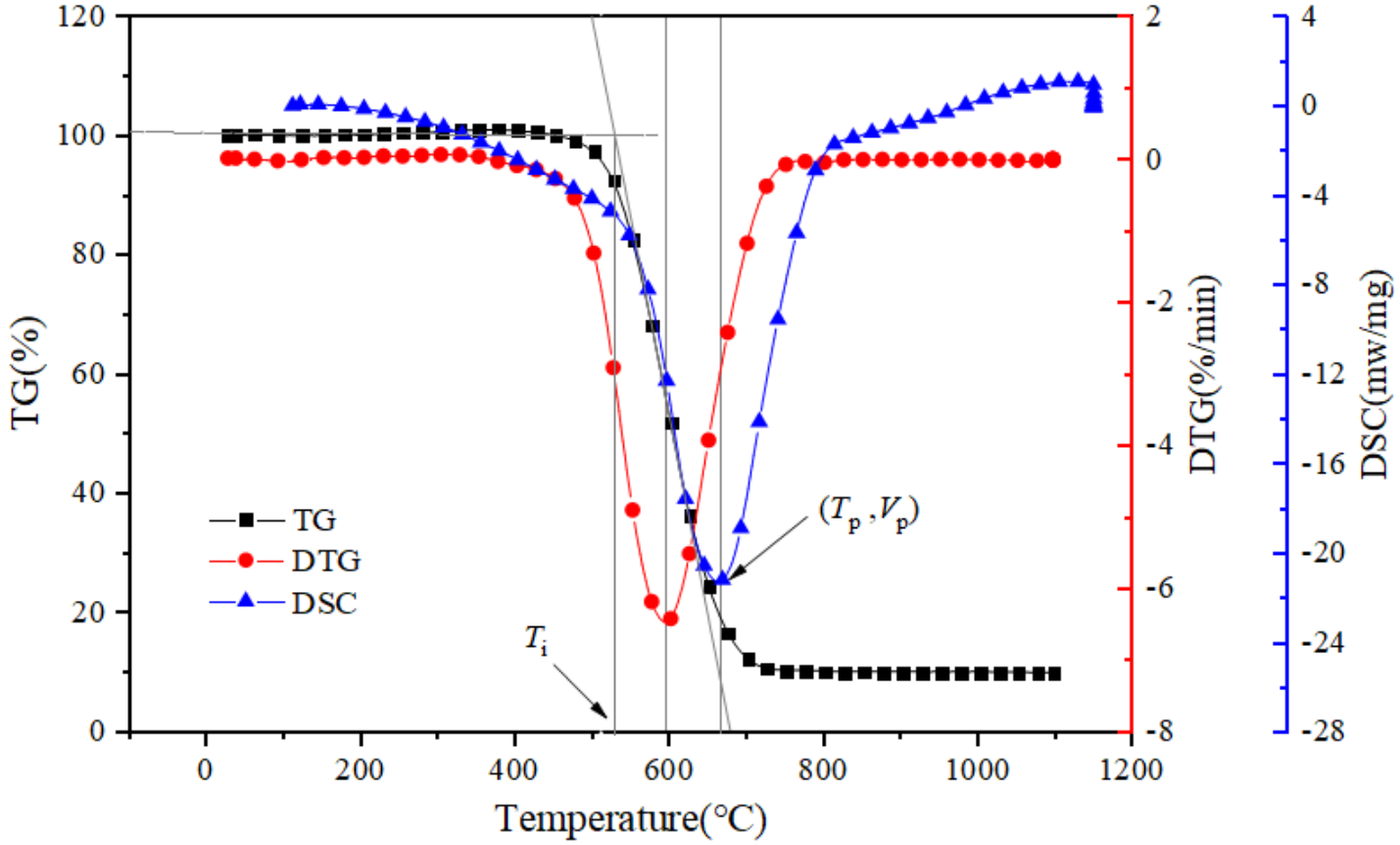

Figure 2

Calculation of combustion characteristic parameters

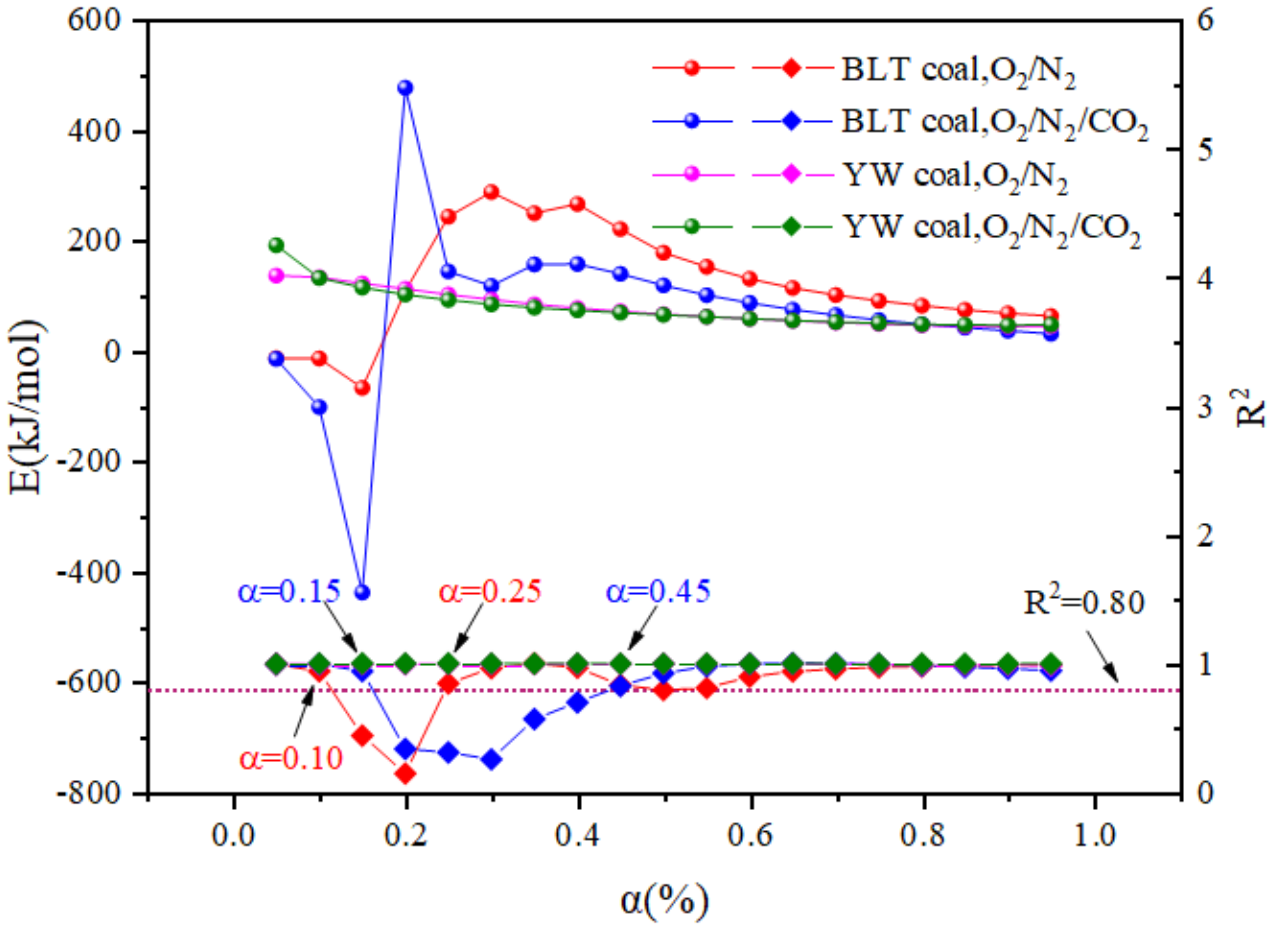

Figure 3

The values of apparent activation energy and R^2 for BLT and YW coal

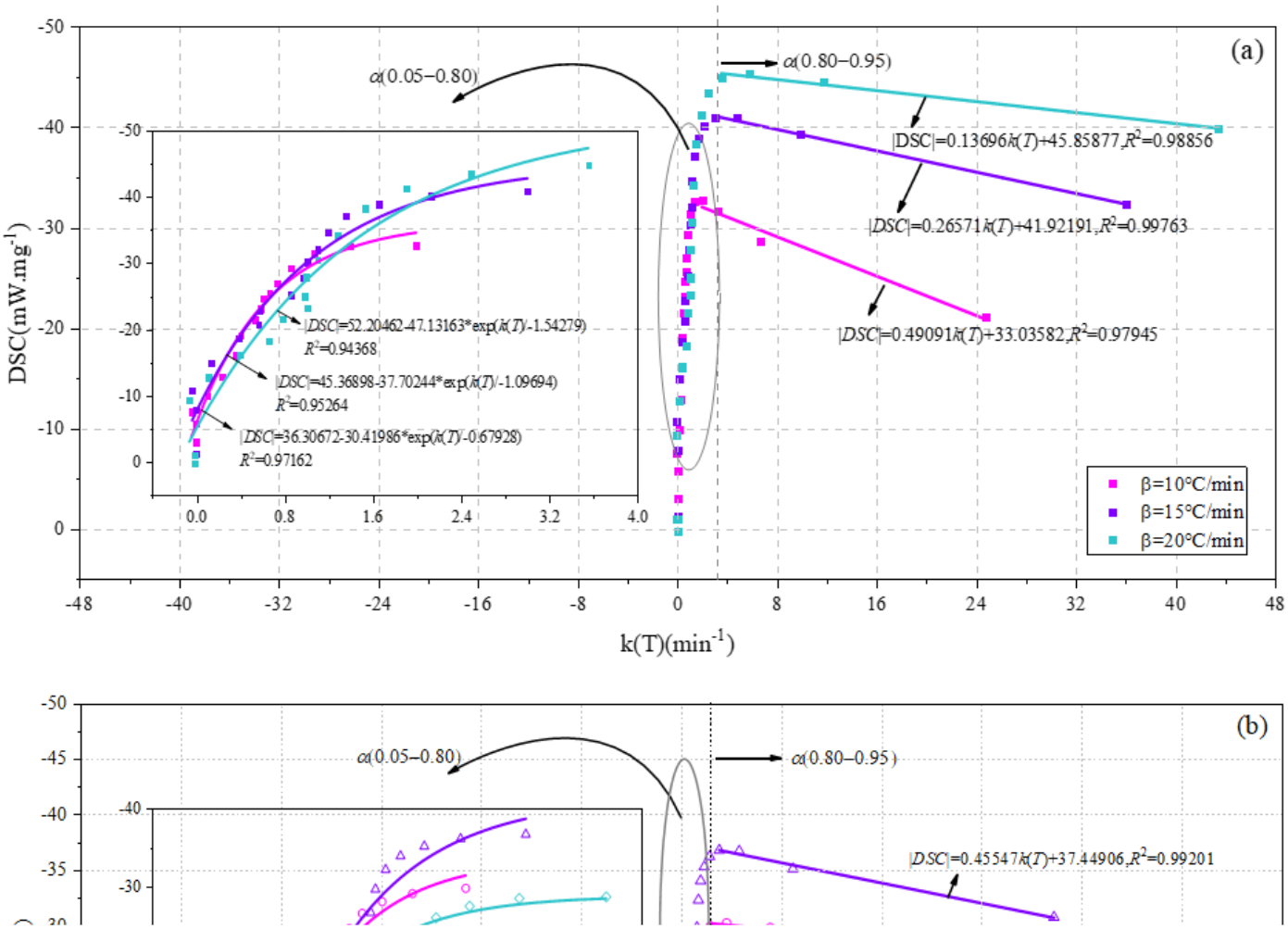

Figure 4

DSC-k(T) curves of BLT coal. (a) O_2/N_2, (b) $O_2/CO_2/N_2$.

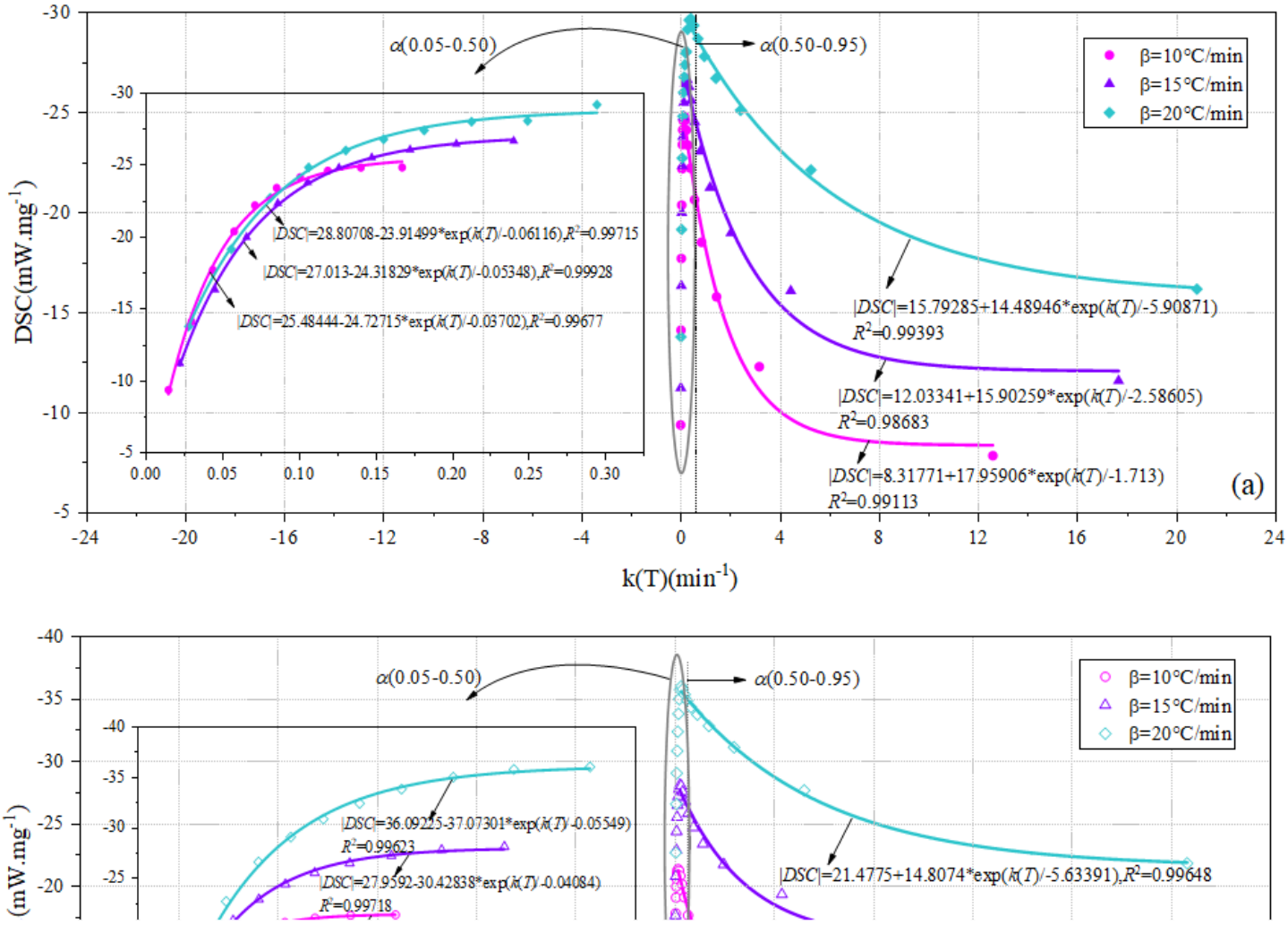

Figure 5

DSC-k(T) curves of YW coal. (a) O_2/N_2, (b) $O_2/CO_2/N_2$.

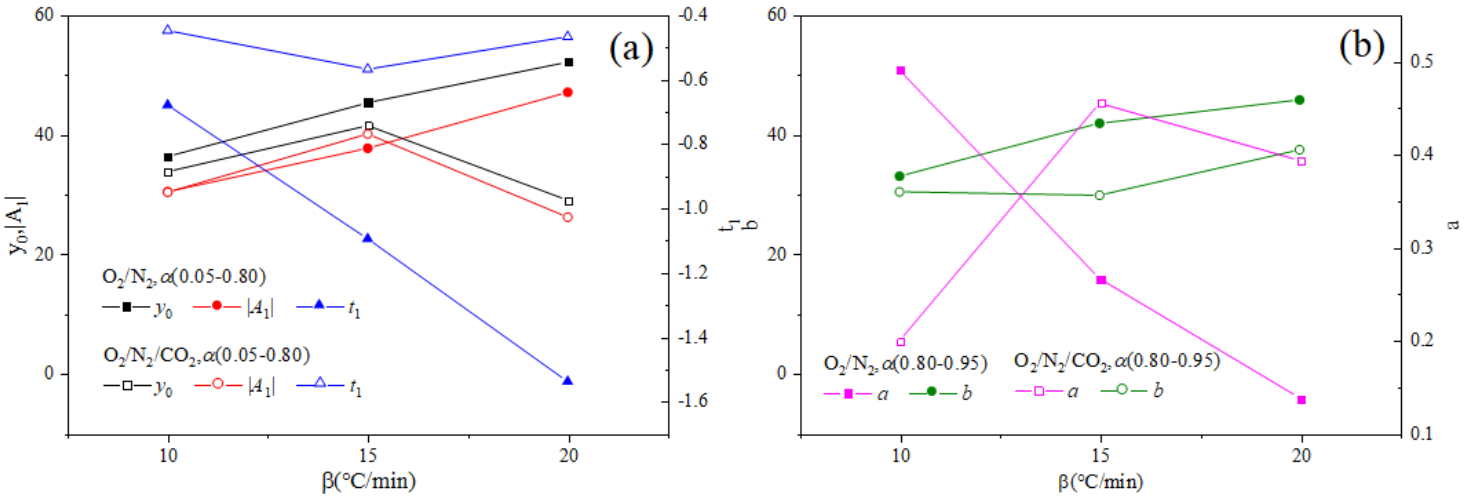

Figure 6

The relationship between y_0, A_1, t_1, a, b and heating rate of BLT coal. (a) α(0.05-0.80), (b) α(0.80-0.95).

Figure 7

The relationship between y_0, A_1, t_1 and heating rate of YW coal. (a) α(0.05-0.50), (b) α(0.50-0.95).